

NASA Technical Memorandum **107602**

107-14
106599
p-31

**GROUND AND FLIGHT CALIBRATION
ASSESSMENT OF HIRAP ACCELEROMETER
DATA FROM MISSIONS STS-35 AND STS-40**

Robert C. Blanchard

Kevin T. Larman

Christina D. Moats

N92-32204

Unclass

63/19 0106599

April 1992



National Aeronautics and
Space Administration

Langley Research Center
Hampton, Virginia 23665-5225

(NASA-TM-107602) GROUND AND FLIGHT
CALIBRATION ASSESSMENT OF HIRAP
ACCELEROMETER DATA FROM MISSIONS
STS-35 AND STS-40 (NASA) 31 p

GROUND AND FLIGHT CALIBRATION ASSESSMENT OF HiRAP ACCELEROMETER DATA FROM MISSIONS STS-35 AND STS-40

Robert C. Blanchard
NASA Langley Research Center
Hampton, Virginia 23665-5225

Kevin T. Larman and Christina D. Moats
Lockheed Engineering & Sciences Company
Hampton, Virginia 23666-1339

Abstract

A method of removing non-aerodynamic signals and calibrating the High Resolution Accelerometer Package (HiRAP) flight data has been developed and is discussed for Shuttle Orbiter missions STS-35 and STS-40. These two mission data sets have been analyzed using ground (dynamic) calibration data and flight calibrations using a flight calibration technique which has been developed and refined over the HiRAP operational lifetime. This technique evolved early in the flight program since it was recognized that ground calibration factors are insufficient to determine absolute low-acceleration levels. The application of flight calibration factors to the data sets from these missions produced calibrated acceleration levels within an accuracy of less than $\pm 1.5 \mu g$ of zero during a time in the flight when the acceleration level was known to be less than $1 \mu g$. This analysis further confirms the theory that flight calibrations are required in order to obtain the absolute measurement of low-frequency, low-acceleration flight signals.

Nomenclature

A	=acceleration measurements, μg
B	=sensor bias
b	=bias coefficient, μg
C	=aerodynamic force coefficient

F	=engineering factor
g	=9.80665 m/s ² , Earth gravitational constant
h	=altitude, km
Hz	=cycles/sec
M	=temperature coefficient, $\mu\text{g}/^{\circ}\text{F}$
m	=orbiter mass
N	=acceleration count measurements
p,q,r	=body angular rates
S	=orbiter reference surface area, (249.9 m ²)
SF	=scale factor
T	=sensor temperature
t	=time
μg	= 1×10^{-6} g
V	=sensor voltage
v	=velocity, m/s
X,Z	=HiRAP sensor location or Orbiter X and Z body axes
ΔA	=incremental acceleration
ρ	=density, kg/m ³
s	=standard deviation

Acronyms

ACIP	=Aerodynamic Coefficient Identification Package
APU	=Auxiliary Power Unit (three separate units)
GMT	=Greenwich Mean Time
HiRAP	=High Resolution Accelerometer Package
OV	=Orbiter Vehicle
OEX	=Orbiter Experiments
STS	=Space Transportation System

Subscripts

1,2	=begin and end of calibration period
76	=1976 U.S. standard atmosphere
c	=calibrated
cg	=with respect to the center of gravity
f	=flight
o	=reference or initial

p =predicted
 u =due to APU

Introduction

Low-frequency, low-acceleration flight measurements have been made by the High Resolution Accelerometer Package (HiRAP) experiment since 1983(1). The HiRAP is a tri-axial, 1×10^{-6} g resolution, pendulous, gas-damped accelerometer installed on the Orbiter with sensor input axes co-aligned to the Orbiter body axes. The HiRAP is designed to measure low-frequency aerodynamic accelerations, and thereby determine Orbiter reentry aerodynamic flight performance characteristics. The HiRAP flight research is a part of the NASA Orbiter Experiments (OEX) program.

Acceleration measurements of low-frequency accelerations, such as aerodynamics, gravity gradient effects, solar radiation pressure, rotational effects, etc., require calibrated signals. Many flight programs rely upon ground calibrations of the accelerometer instrument system in a 1 g environment to provide the necessary factors to properly adjust the flight measurements in a μ g environment. It was recognized early in the HiRAP flight program that ground calibration factors were not producing the desired flight results. Initially, it was theorized that "dynamic" temperature effects were a major contributor to the problem. Static ground calibrations (i.e., stabilize the temperature of the laboratory sensor equipment, and its surroundings before taking the calibration data) were replaced by "dynamic" calibrations. Dynamic calibrations include ramping the temperature of the equipment to the anticipated flight temperature profile while collecting the calibration factors.

This paper presents an overview of two methods used to calibrate HiRAP's low-frequency, low acceleration data on missions STS-35 and STS-40. Also presented are the results of an assessment of dynamic ground and flight calibration factors using flight data from each of these

missions. The two mission data sets discussed compliment data from 10 prior missions. (2)

Analysis of Flight Data

HiRAP science count data, measurements of acceleration from each of the three sensors, and housekeeping data, measurements of sensor temperature and power supply voltages, are recorded as a function of Greenwich Mean Time (GMT). The science count data are collected at a rate of 112.6 Hz and the housekeeping data are at a rate of 2.7 Hz. An example of these acceleration data for the X and Z- axes is presented in Fig. 1, which shows acceleration count data versus GMT for STS-35. The large spikes in the data followed by damping are examples of thruster induced accelerations. These non-aerodynamic accelerations are removed from the data along with the rotational induced linear accelerations using ancillary data. Once these non-aerodynamic components are removed, the data are averaged into a 1 Hz uncalibrated aerodynamic data set.

Aerodynamic Acceleration Determination

The method used to convert the acceleration count values (N_i) into engineering units is:

$$\begin{aligned} V_i &= -10 + (N_i/16383)*20 & (\text{volts}) \\ A_i &= V_i/SF_i & (\mu g) \end{aligned} \quad (1)$$

where $i=X,Z$, and where,

$$\begin{aligned} SF_x &= -.0012466 & (\text{volts}/\mu g) \\ SF_z &= -.0012477 & (\text{volts}/\mu g) \end{aligned} \quad (2)$$

Figure 2 shows an example of the converted HiRAP data for STS-35. Since the HiRAP is not located on the center of gravity of the Orbiter Vehicle (OV), rotational motions about the OV center of gravity will induce non-aerodynamic linear accelerations. The following equations are used to correct for the induced accelerations in the data:

$$\begin{bmatrix} \Delta A_x \\ \Delta A_z \end{bmatrix} = \begin{bmatrix} -(q^2 + r^2) & pq & pr \\ pr & qr & -(q^2 + p^2) \end{bmatrix} \begin{bmatrix} X_{cg} \\ Y_{cg} \\ Z_{cg} \end{bmatrix} \quad (3)$$

$$\begin{bmatrix} A_x \\ A_z \end{bmatrix}_{cg} = \begin{bmatrix} A_x \\ A_z \end{bmatrix} - \begin{bmatrix} \Delta A_x \\ \Delta A_z \end{bmatrix} \quad (4)$$

where p,q, and r are the OV body axis angular rates. The corresponding angular accelerations are not included in the above Eq. (3) since their contributions are relatively small. Figure 3 shows the magnitude of the corrections (i.e., equation (3) values) for STS-35. As seen, the contributions for this flight regime are less than $\pm 2 \mu g$.

The thrust induced signals are removed from the data set by deleting the data in the time frames of thruster activity. Then, after thrust removal and center of gravity adjustments (when required), a one sec average of the acceleration data set is made. This one second average data set represents the uncalibrated acceleration data due to aerodynamic accelerations, as shown in Fig. 4. These data are now in a form to be calibrated since the only component of significance is the aerodynamic signal which can be bounded in magnitude.

Ground Calibration

Ground calibrations of the HiRAP instrument began in 1981(3). A second calibration occurred in 1985(4). An example of the static temperature coefficient data for the X-axis sensor is shown in Fig. 5. The early development ground calibrations were extensive, providing both bias and scale factor values as a function of temperature in an attempt to predict the sensor behavior in flight. However, the results of applying the static calibration factors to the flight data always required additional biasing (and in some instances changing the sensor temperature coefficient) to achieve the correct acceleration levels.

After several flights of the HiRAP, a ground calibration which more closely simulated flight conditions was devised. That is, in 1989 (5) a calibration procedure was generated to simulate the change in temperature of the sensor based upon prior flight experience. This is referred to as a "dynamic" calibration.

A summary of the 1989 temperature coefficient data for the X and Z axes is presented in Fig. 6 and Fig. 7, respectively. Applying the dynamic calibration factors to the uncalibrated aerodynamic data sets for STS-35 and STS-40 produces the results in Fig. 8. The altitude and attitude of the OV during this particular data segment indicates that no aerodynamic accelerations are detectable by the HiRAP. In addition, the crew is seated and prepared for reentry, the thrust induced signals have been accounted for, and the Auxiliary Power Unit (APU) average acceleration signal is known to be about $17 \mu g$ per APU. As an example, for STS-40, the indicated acceleration and residual temperature coefficient is on the order of $100 \mu g$ and $0.66 \mu g/^\circ F$ for the X-axis, and $300 \mu g$ and $.57 \mu g/^\circ F$ for the Z axis. Like the static ground calibration, the dynamic ground calibration is insufficient in determining the absolute measurement of low-frequency, low-acceleration signals.

The dynamic ground calibration does, however, examine instrument responses as if in a flight mode. This allows a good understanding of the overall temperature response of the instrument and isolates anomalies, for example, the disjoint at $120^\circ F$ for the current HiRAP sensors. In addition, the sensor temperature coefficient (i.e., the change in bias due to temperature change) is predicted to within $1.5 \mu g/^\circ F$ by the dynamic ground calibration. This data are useful in characterizing accelerometer behavior in a noisy environment, such as, the HiRAP Z-axis when all three APUs are active.

Flight Calibration

The approach of the flight calibration method is to determine an OV altitude and attitude at which the acceleration levels are less than

1 μg and use HiRAP flight acceleration and temperature data to characterize the sensor biases. Once the model has predicted the minimum altitude below which calibration cannot be performed, a data set for each axis is chosen on which to calculate the bias values. In the case of the X- axis, the predicted altitude or above is used. In the case of the Z-axis, a combination of pre- and post-APU transition data segments is used. Once the segments have been located, a linear regression of sensor acceleration and temperature data are computed. The uncertainties in the regression components are used to determine the overall calibration uncertainty.

The "zero-g" model is composed of the 1976 U.S. standard atmosphere (6) and the OV aerodynamics(1)(7)(8)(9). The predicted acceleration is calculated by:

$$A_{pi} = (F_i)(1/2)(C_i)(\rho_{76})(v^2)(S/m) \quad (5)$$

where $i = x, z$ and F_i is the engineering factor safety margin, or degree of conservatism used to account for deviations in atmosphere and/or aerodynamics for any given flight. From HiRAP experience to date, $F=2$ is more than adequate. The aerodynamic coefficients, C_i , include a rarefied-flow regime model developed from the HiRAP flights (see Ref. 2). The results of the calculations for missions STS-35 and STS-40 are shown in Fig. 9 and Fig. 10, respectively. The latest time segment of available flight data which is predicted to measure less than 1 μg is used for each sensor in the determination of the calibration factors. The temperature segments used in the calibration are shown for both flights in Fig. 11. The linear regression of sensor acceleration with sensor temperature produces a bias calibration of the form:

$$B_{fi} = M_i(T_i - T_{oi}) + b_i \quad (6)$$

where $i=x, z$. The results of the flight calibration and uncertainty values determined by the linear regression are presented in Tables I and II, respectively. These bias values are removed from the uncalibrated aerodynamic data using:

$$A_{ci} = A_i - B_{fi} \quad (7)$$

where $i=x,z$. The results of applying the flight calibration technique are presented in Fig. 12 and Fig. 13.

After the flight bias values are removed, the aerodynamic accelerations are very near zero during the calibration interval. The three APU exhaust ports are located at the tail of the OV such that a non-aerodynamic acceleration is induced along the Z-axis only. The flight calibration requires that the bias slope and bias of the data be known. Sometimes, the second and third APUs are turned on after the chosen calibration segment. The effect of the added exhaust thrust is to create a step function in the acceleration level. This step must be determined in order to correctly account for the Z-axis aerodynamic data during the rest of the descent. This is performed by determining the best fit lines through the data just before and just after the APU transition, evaluating the two lines at the place where the APU transition occurs, and calculating the difference. This difference is incorporated into the calibration factors determined just before the APU transition to complete the bias determination for the Z-axis data following the last APU transition. That is,

$$A_{cz} = A_z - B_{fz} + \Delta A_{uz} \quad (8)$$

where ΔA_{uz} is the acceleration increment due to the APU. This process is shown in Fig. 14 and Fig. 15 for STS-35 and STS-40, respectively. The value of ΔA_{uz} for STS-35 is 34 μg and 33 μg for STS-40. The flight and ground calibration factors are presented in Table I.

Calibration Uncertainty Estimates

An error analysis was performed on the two flight data sets. The details, including selected calibration time interval, sensor temperatures during flight, and linear regression factors with their accompanying uncertainty coefficients are included in Table II. Table III represents a

summary comparison of the calibrated signals and relative uncertainties of the two calibration methods discussed in this report. For each column, for a given flight, the first entry is the acceleration value obtained by the the respective calibration technique. For instance, on mission STS-35, the flight calibration technique produces an acceleration of $0.0 \mu\text{g}$ for both X and Z sensors, while for the same period of time in the flight the ground calibrations produce -81 and $-282 \mu\text{g}$ accelerations in the X and Z sensors, respectively. In the parenthesis are the estimates of the uncertainties associated with the temperature coefficient and the bias for each sensor and each technique. The flight calibration uncertainty in the Z-axis is analyzed with two segments (i.e., from one APU to three APU active) and thus, the total uncertainty shown accounts for both error sources by combining, in a root sum square fashion, the contributions from each. The ground calibration errors are representative of the scatter in the laboratory data and obviously are optimistic estimates if applied directly to the flight data. Clearly the effects of measurements in a 1 g environment are not applicable to a μg environment even though the uncertainties do not reflect this fact.

Summary

The ground calibration evolution, beginning with static and currently at dynamic, devised to permit the interpretation of low-frequency, low acceleration flight data from the HiRAP instrument has not been satisfactory. A flight calibration method was developed to overcome this inadequacy. The two calibrations, both ground and flight, were applied to the STS-35 and STS-40 data sets and compared. The results using flight calibrations were within the expected levels of measurement whereas the dynamic ground calibration results were not. For example, on STS-35 and 40, acceleration levels between -81 and $-355 \mu\text{g}$ were found after application of ground calibrations during a time in the flight when acceleration levels were known to be less than $1 \mu\text{g}$. Despite significant improvements in ground calibration, satisfactory results are not currently possible. This may be a universal

problem due perhaps to the problems of calibrating at μg levels while in a 1-g field. The results of these analyses indicate that a method of in-flight calibration of low-frequency, low acceleration measurements is required. The flight calibration technique presented satisfactorily resolves issues for the HiRAP experimentation. However, until insitu self-calibrating instrumentation becomes proven and technically acceptable, it is highly likely that other μg instrumentation will need to address the issue of ground to flight calibration applicability.

References

(1) Blanchard, R. C.; and Rutherford, J. F.: Shuttle Orbiter High Resolution Accelerometer Package Experiment: Preliminary Flight Results. Journal of Spacecraft and Rockets, vol. 22, no. 4, July-August 1985, pp. 474-480.

(2) Blanchard, R. C., Larman, K.T., Barrett, M.: The High Resolution Accelerometer Package (HiRAP) Flight Experiment Summary for the First Ten Flights, NASA RP-1267, March 1992.

(3) KMS Fusion Report No. KTR-102, "Proposed Algorithms for Computing HiRAP Temperatures and Temperature Effect Corrections," KMS Fusion, Inc., August 1982.

(4) KMS Fusion Report No. KTR-105, "HiRAP S/N-001 Calibration Analysis Report," KMS Fusion, Inc., March 1985.

(5) "HiRAP S/N 001 Calibration Analysis Report," KTR-184, KMS Fusion, Inc., September 1989.

(6) U.S. Standard Atmosphere, 1976 NOAA, NASA, USAF, Oct. 1976.

(7) Aerodynamic Design Data Book. Volume 1-Orbiter Vehicle, 1978: Part 1, NASA CR-171859, 1978 (revised Apr. 1982). Part 2, NASA CR-171854, 1978 (revised Apr. 1982).

(8) "Flight Assessment Package Orbiter Aerodynamics," FAD-26, April 1986, NASA JSC-22078.

(9) Blanchard, R.C., Hinson, E.W., Nicholson, J.Y.: Shuttle High Resolution accelerometer Package Experiment Results: Atmospheric Density Measurements between 60-160 km, Journal of Spacecraft and Rockets, vol. 26, no. 3, May-June 1989, pp. 173-180.

Table I. Comparison of Calibration Factors.

X-AXIS	STS-35	
	1989 GROUND BIAS, μg	FLIGHT BIAS, μg
	$-25.75(T_x - 70.42) + 752.61$	$-24.72(T_x - 70.42) + 682.91$
Z-AXIS	$-22.27(T_z - 69.61) - 981.66$	$-22.89(T_z - 69.61) - 1280.33$
Z-AXIS post-APU		$-22.89(T_z - 69.61) - 1314.33$
STS-40		
X-AXIS	1989 GROUND BIAS, μg	FLIGHT BIAS, μg
	$-25.75(T_x - 67.67) + 752.61$	$-25.05(T_x - 67.67) + 726.90$
	Z-AXIS	$-21.98(T_z - 66.89) - 1257.80$
	$-22.27(T_z - 69.61) - 981.66$	
Z-AXIS post-APU		$-21.98(T_z - 66.89) - 1290.80$

Table II. Linear Regression Values and Uncertainty Coefficients

	STS-35			STS-40		
	X	Z (PRE-APU)	Z (POST-APU)	X	Z (PRE-APU)	Z (POST-APU)
t_1	18501	18501	18800	53455	53455	53819
t_2	18801	18601	19100	53706	53706	53931
M	-24.72	-22.89	-22.89	-25.05	-21.98	-21.80
σ_M	1.18	2.89	1.29	0.95	0.58	5.79
b	682.91	-1280.33	-1277.45	726.90	-1257.80	-1260.48
σ_b	0.83	0.71	0.95	0.61	0.37	1.44
T_1	70.42	69.61	70.97	67.67	66.89	68.52
T_2	71.79	70.06	72.42	68.84	68.04	68.99

Table III. Comparison of Uncertainty Estimates.

	FLIGHT	GROUND
	STS-35	1989
X-AXIS	0.0 μg ($\pm 1.18\mu\text{g}/^\circ\text{F} \pm 0.83\mu\text{g}$)	-81 μg ($\pm 1.51 \mu\text{g}/^\circ\text{F} \pm 1.14 \mu\text{g}$)
Z-AXIS	0.0 μg ($\pm 2.89\mu\text{g}/^\circ\text{F} \pm 1.19\mu\text{g}$)	-282 μg ($\pm 11.25 \mu\text{g}/^\circ\text{F} \pm 2.63 \mu\text{g}$)
	STS-40	1989
X-AXIS	0.0 μg ($\pm 0.95\mu\text{g}/^\circ\text{F} \pm 0.61\mu\text{g}$)	-96 μg ($\pm 5.11 \mu\text{g}/^\circ\text{F} \pm 2.47 \mu\text{g}$)
Z-AXIS	0.0 μg ($\pm 0.58\mu\text{g}/^\circ\text{F} \pm 1.49\mu\text{g}$)	-355 μg ($\pm 4.94 \mu\text{g}/^\circ\text{F} \pm 2.18 \mu\text{g}$)

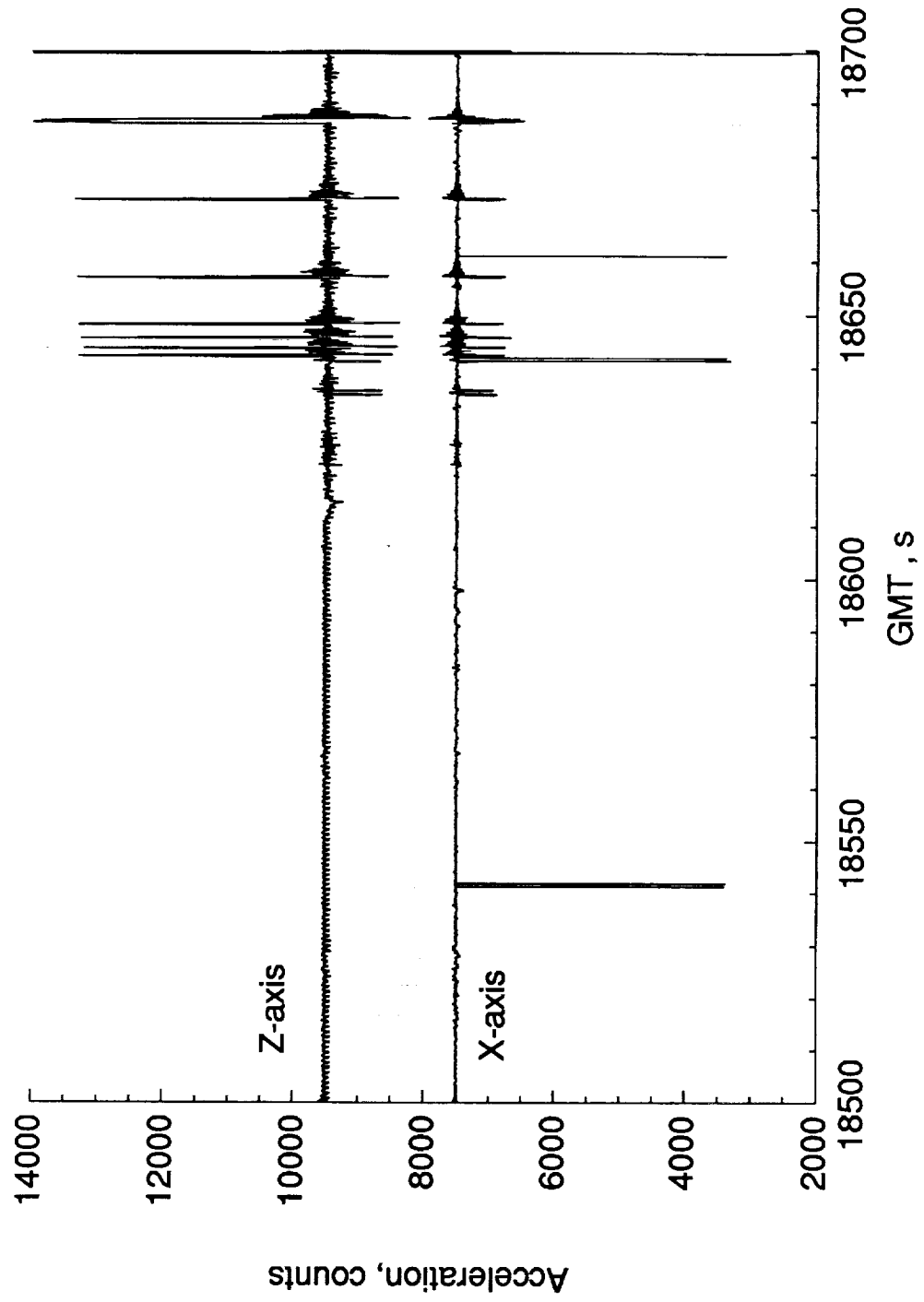


Figure 1. HiRAP Count Data for STS-35 Flight Segment

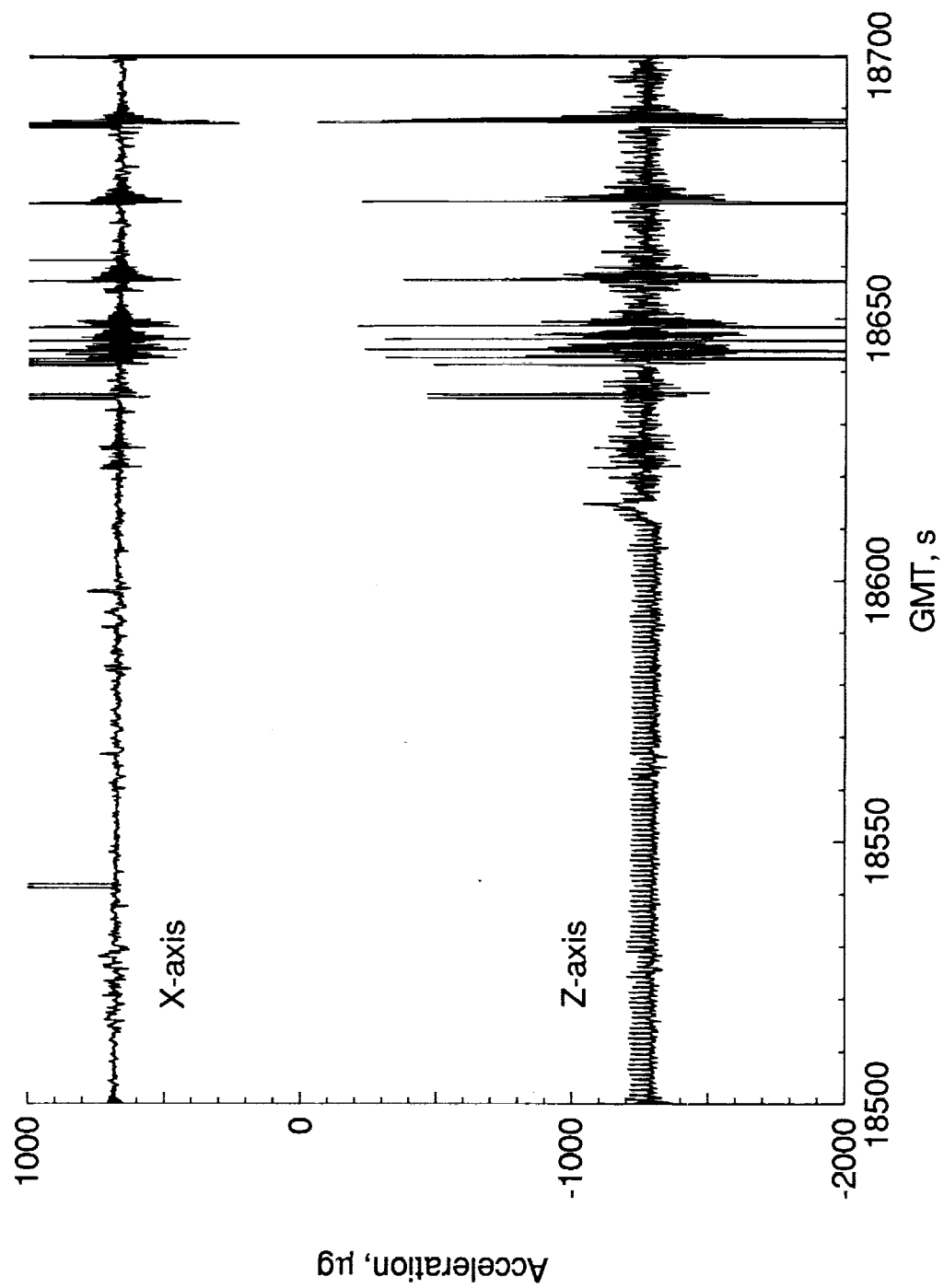


Figure 2. HIRAP Acceleration Data for STS-35 Flight Segment

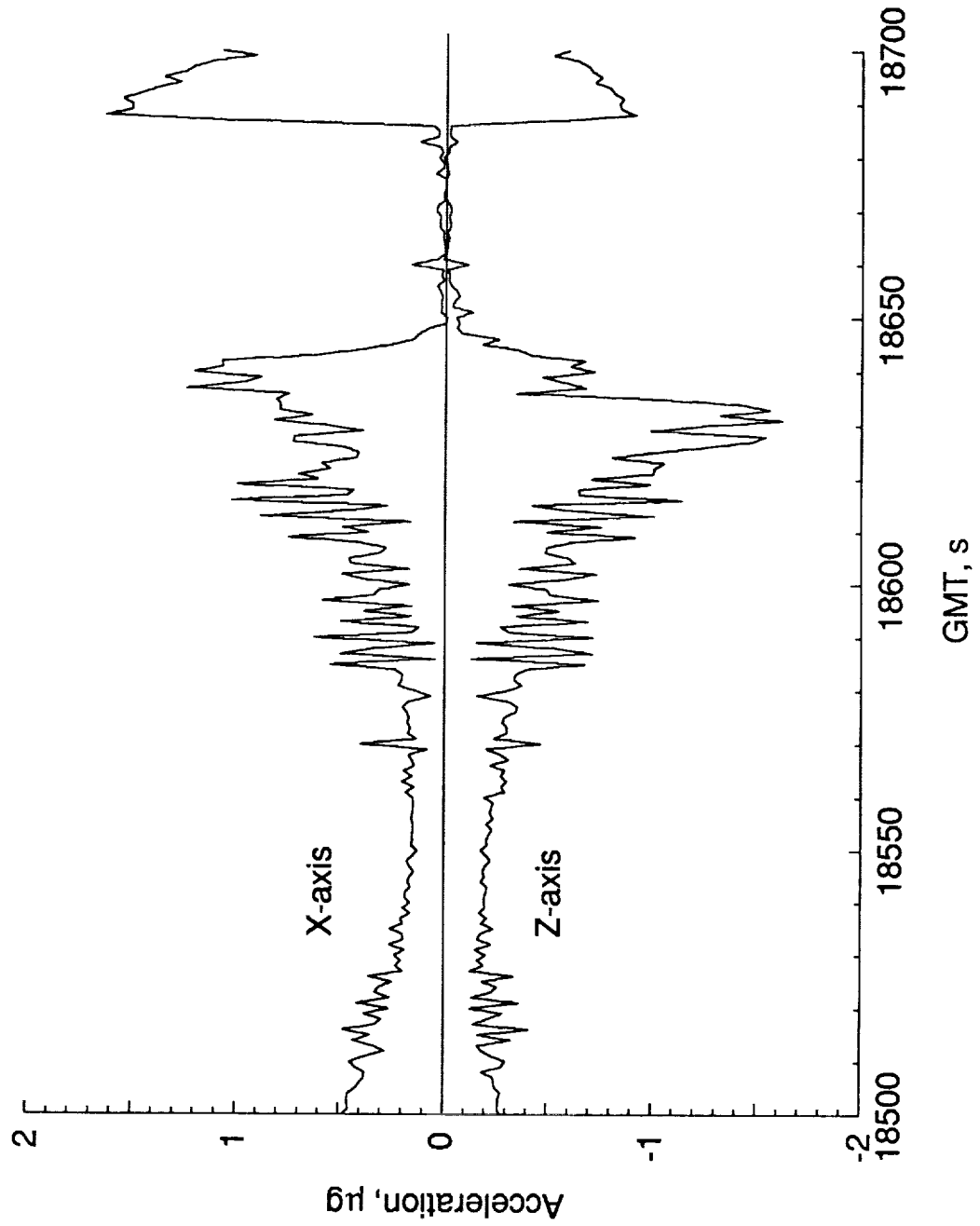
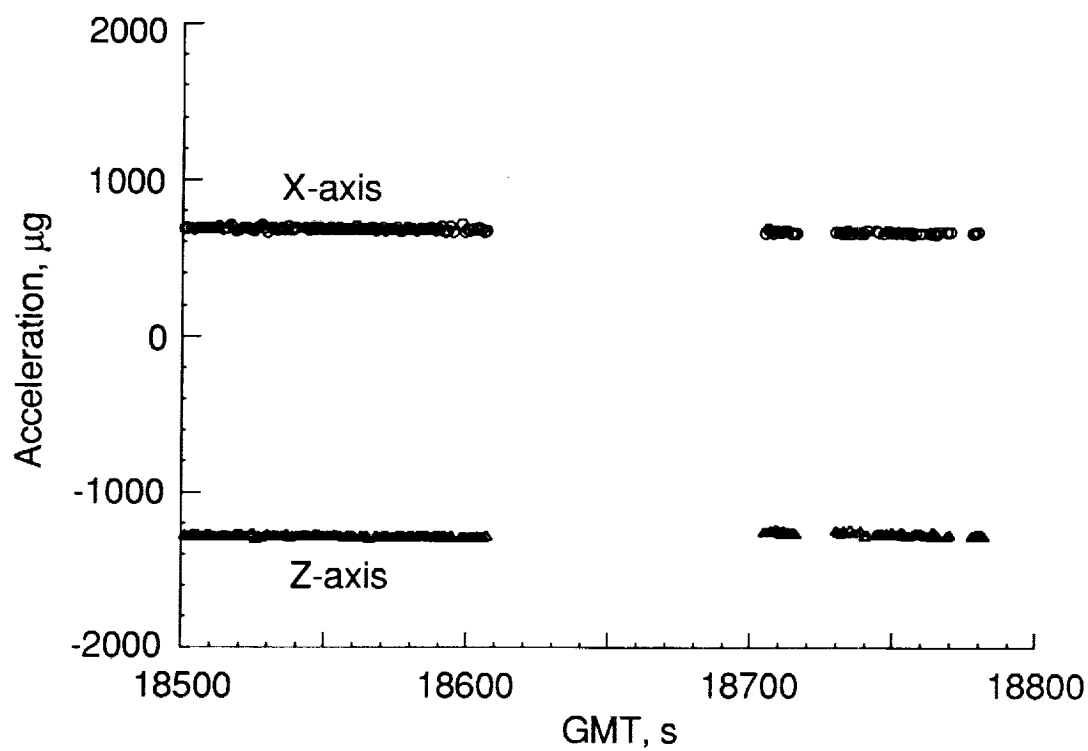
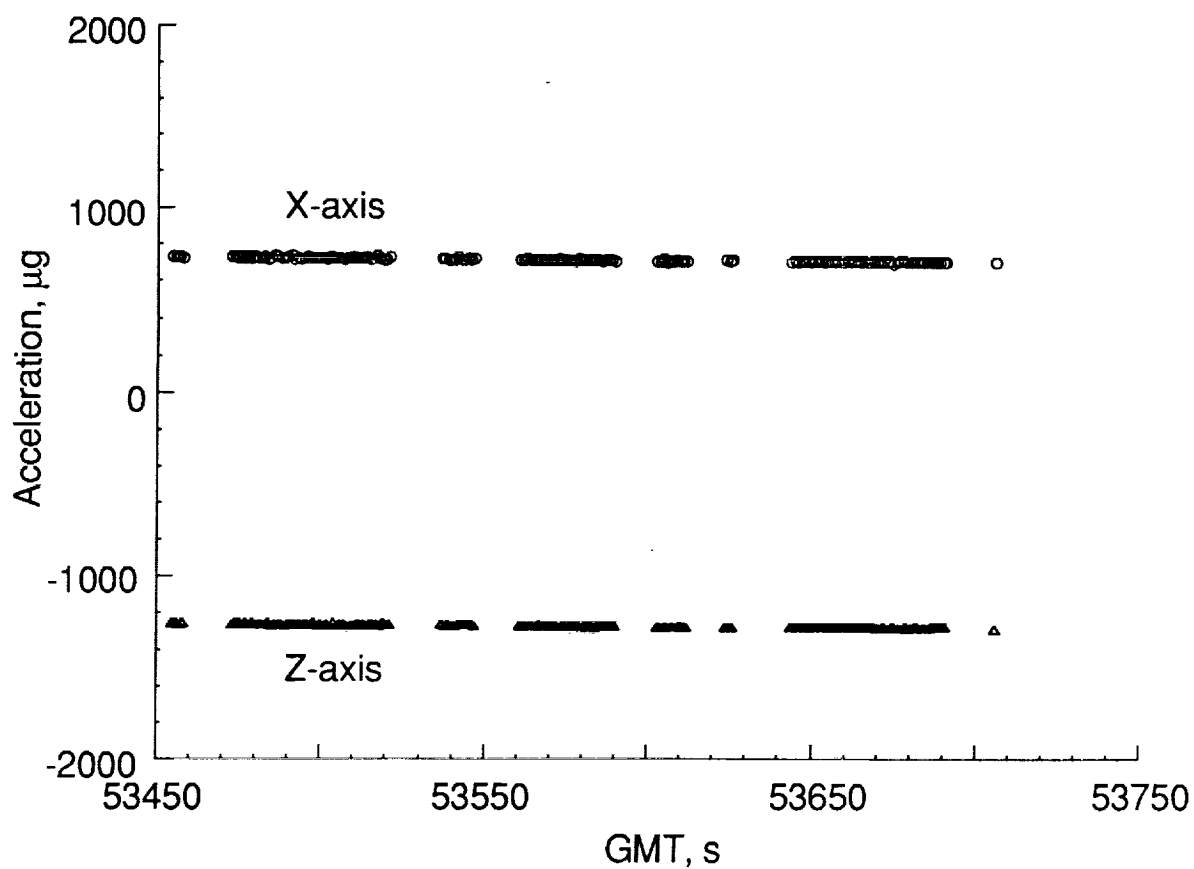


Figure 3. HIRAP STS-35 Linear Induced Accelerations



(a) HiRAP STS-35 Data



(b) HiRAP STS-40 Data

Figure 4. HiRAP Uncalibrated Acceleration Data.

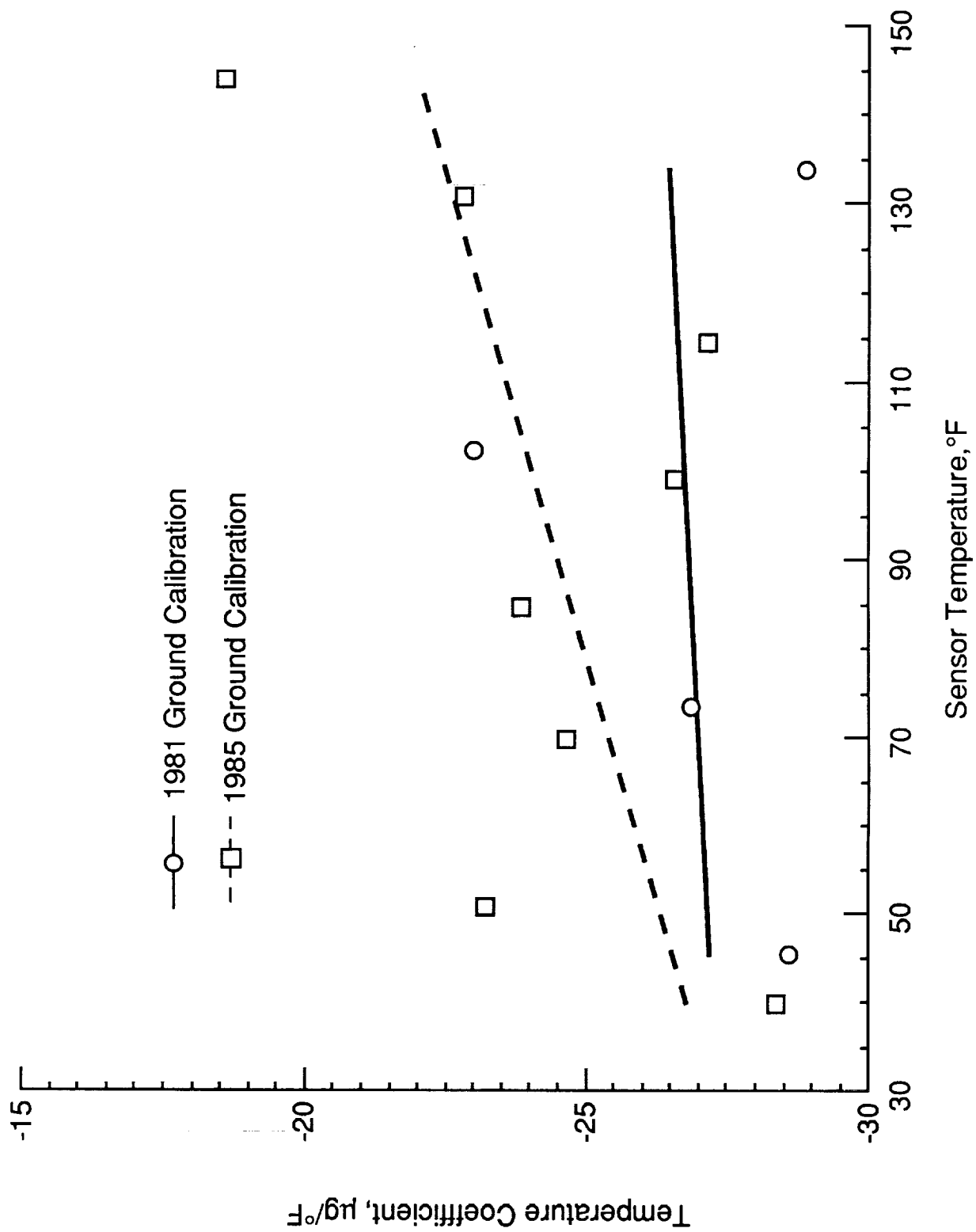


Figure 5. HiRAP X-axis Static Calibration Data.

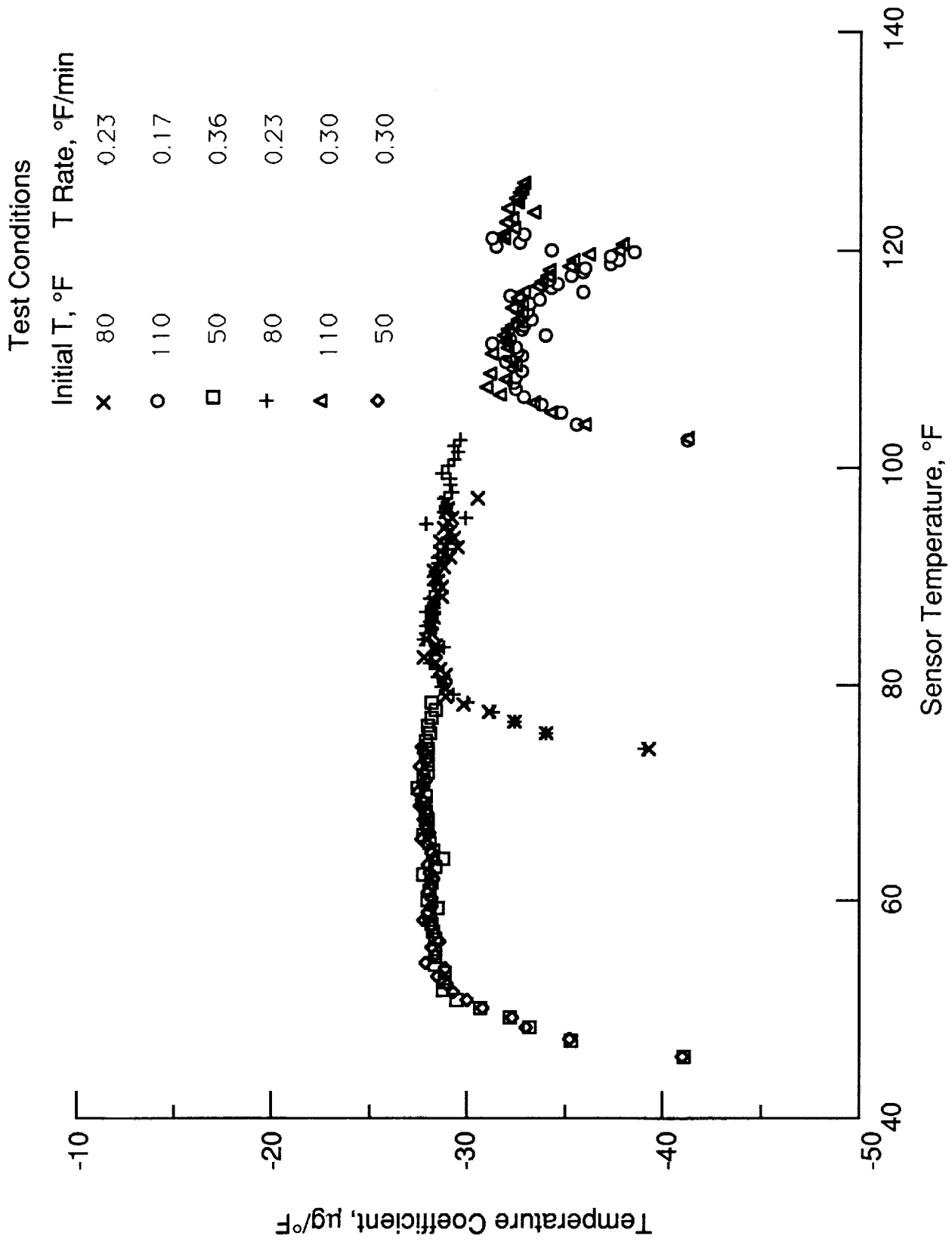


Figure 6. HiRAP X-sensor Ground Calibration Data(1989 Dynamic).

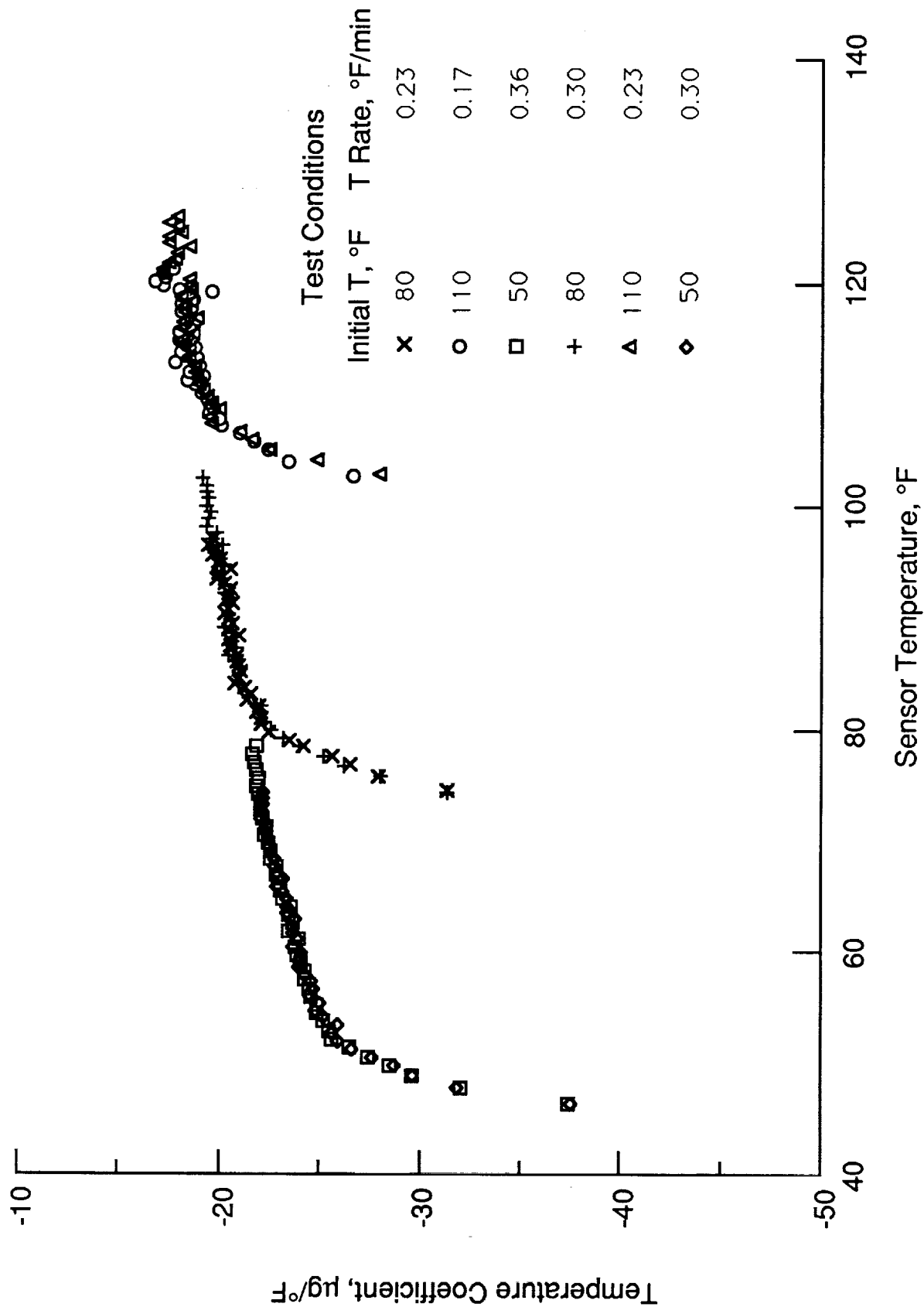
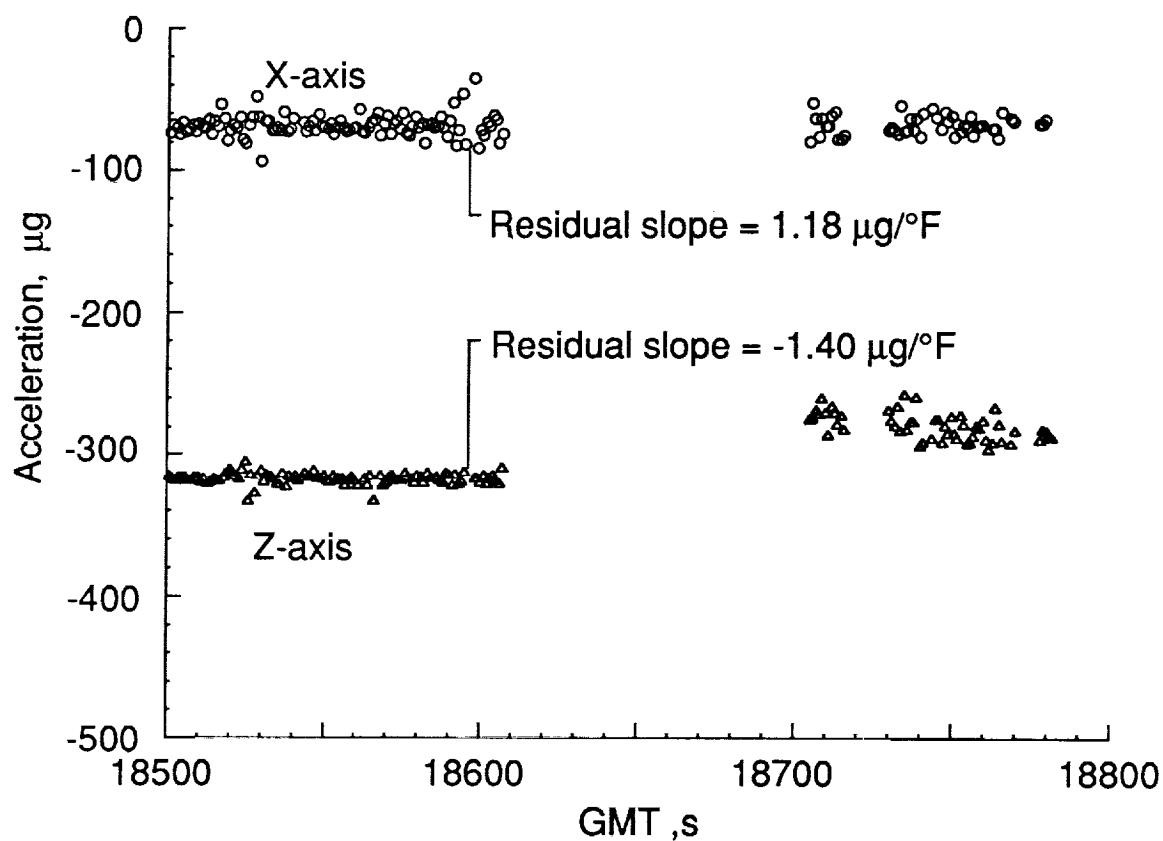
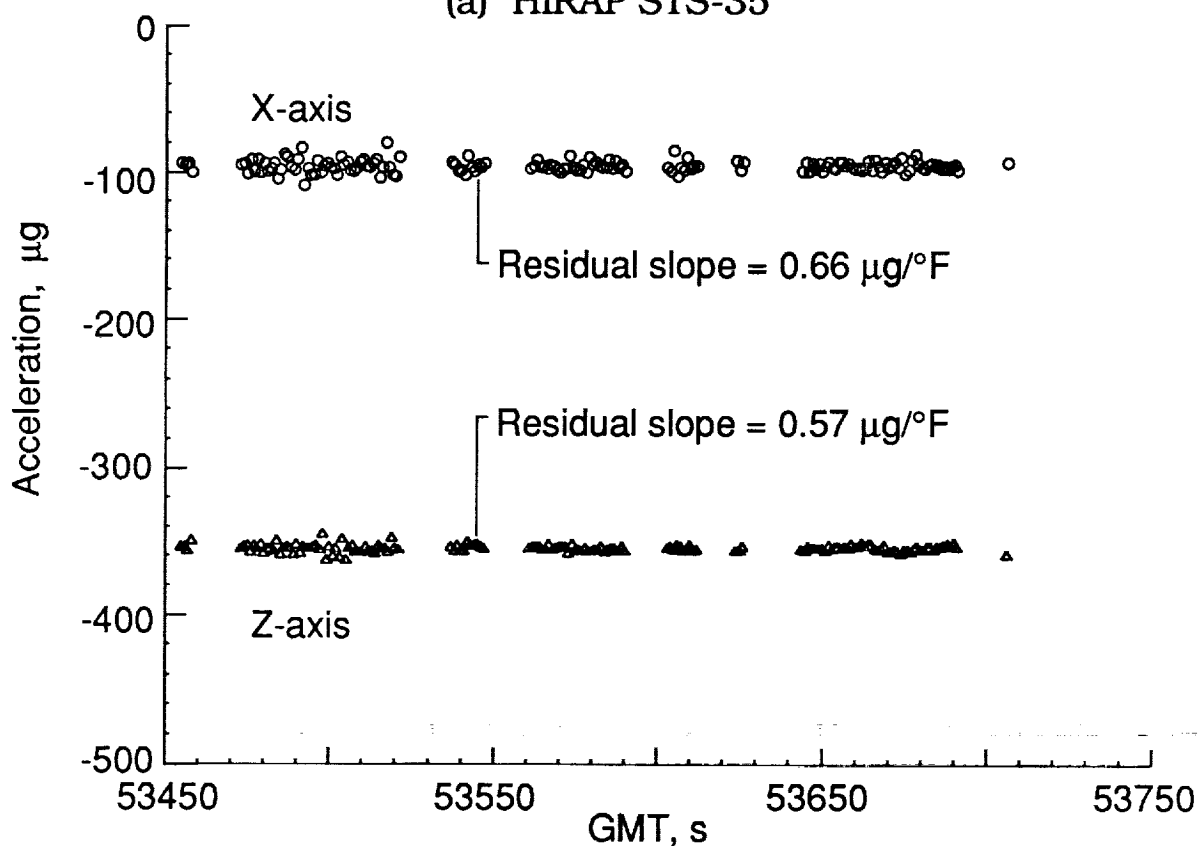


Figure 7. HiRAP Z-sensor Ground Calibration Data(1989 Dynamic).



(a) HiRAP STS-35



(b) HiRAP STS-40

Figure 8. HiRAP Ground Dynamic Calibrated Data

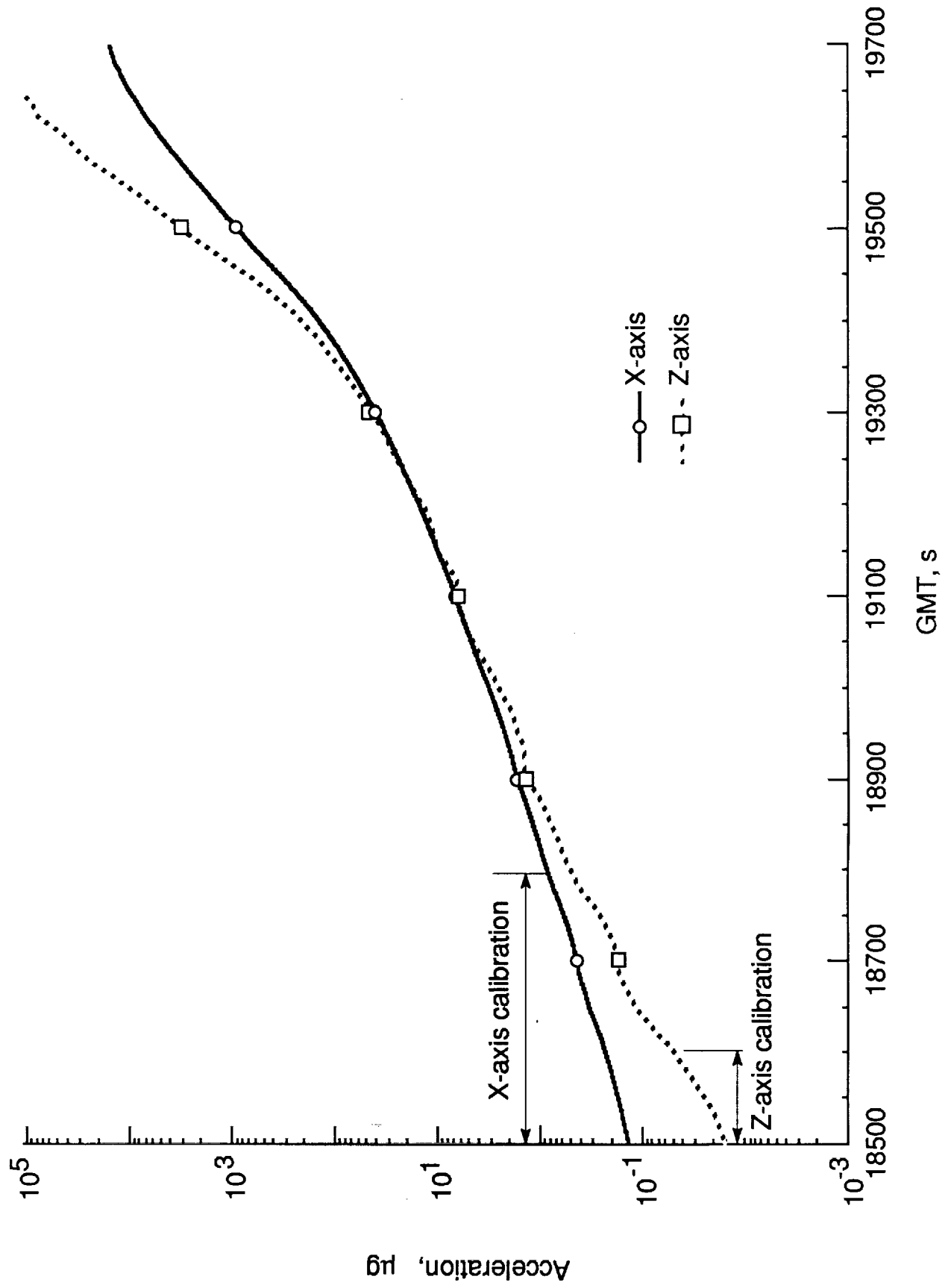


Figure 9. HiRAP STS-35 Acceleration Model Results.

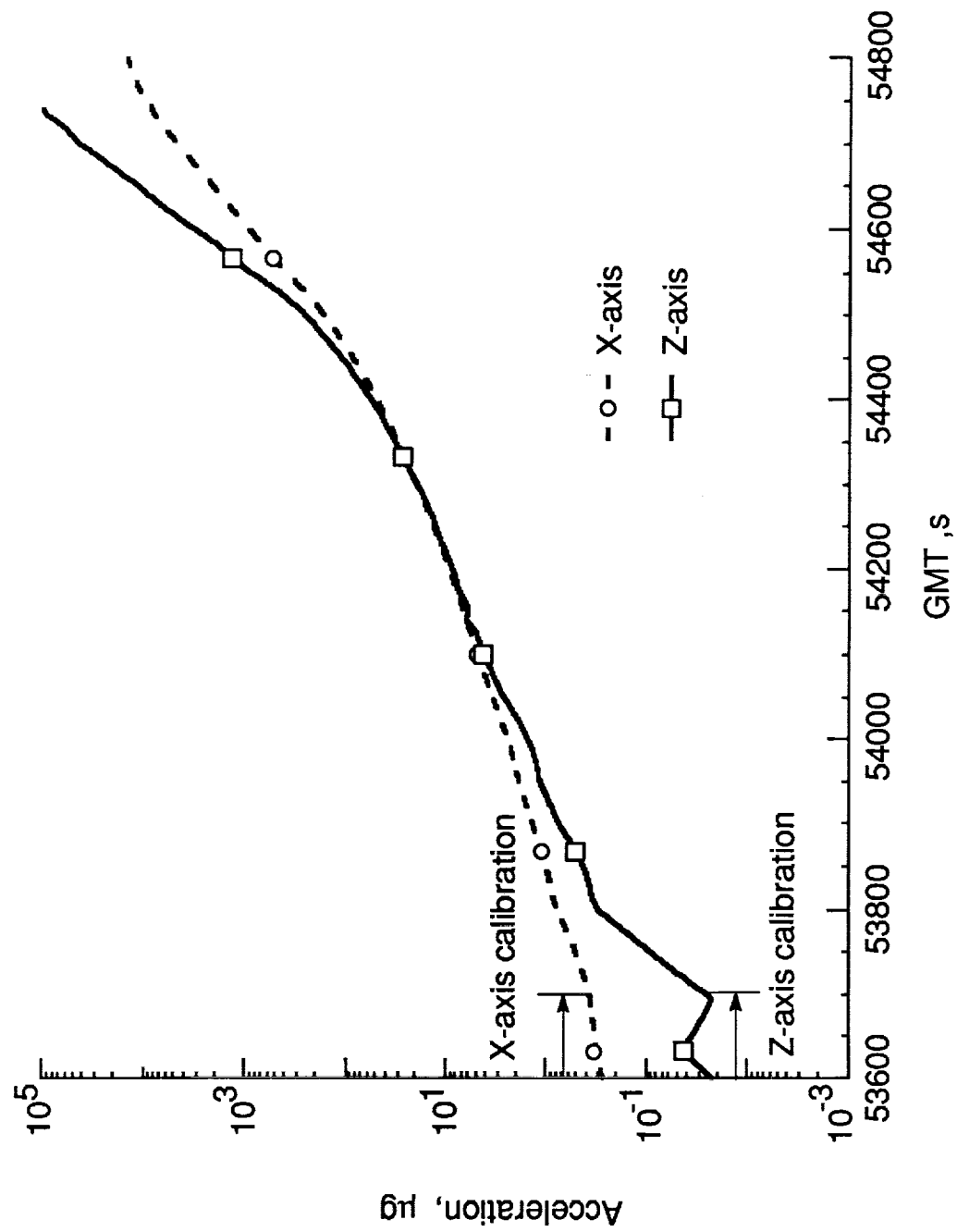
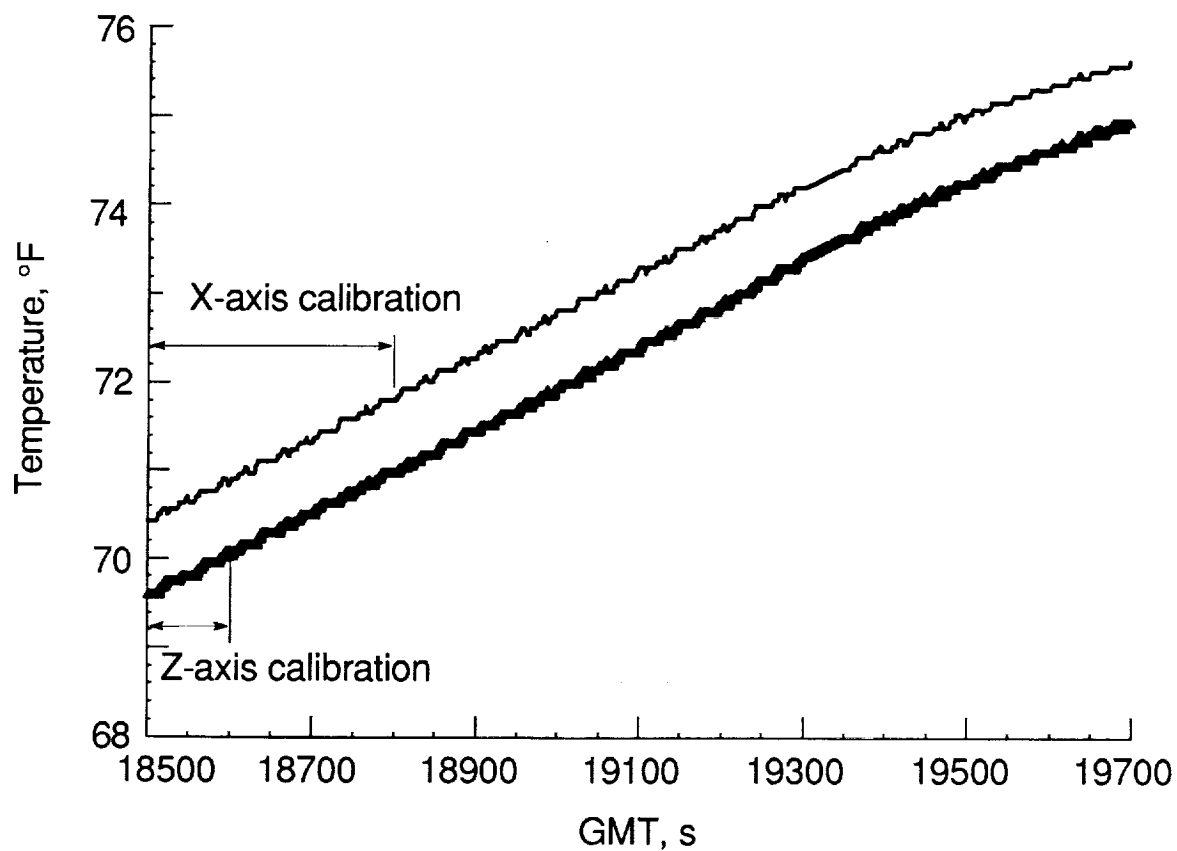
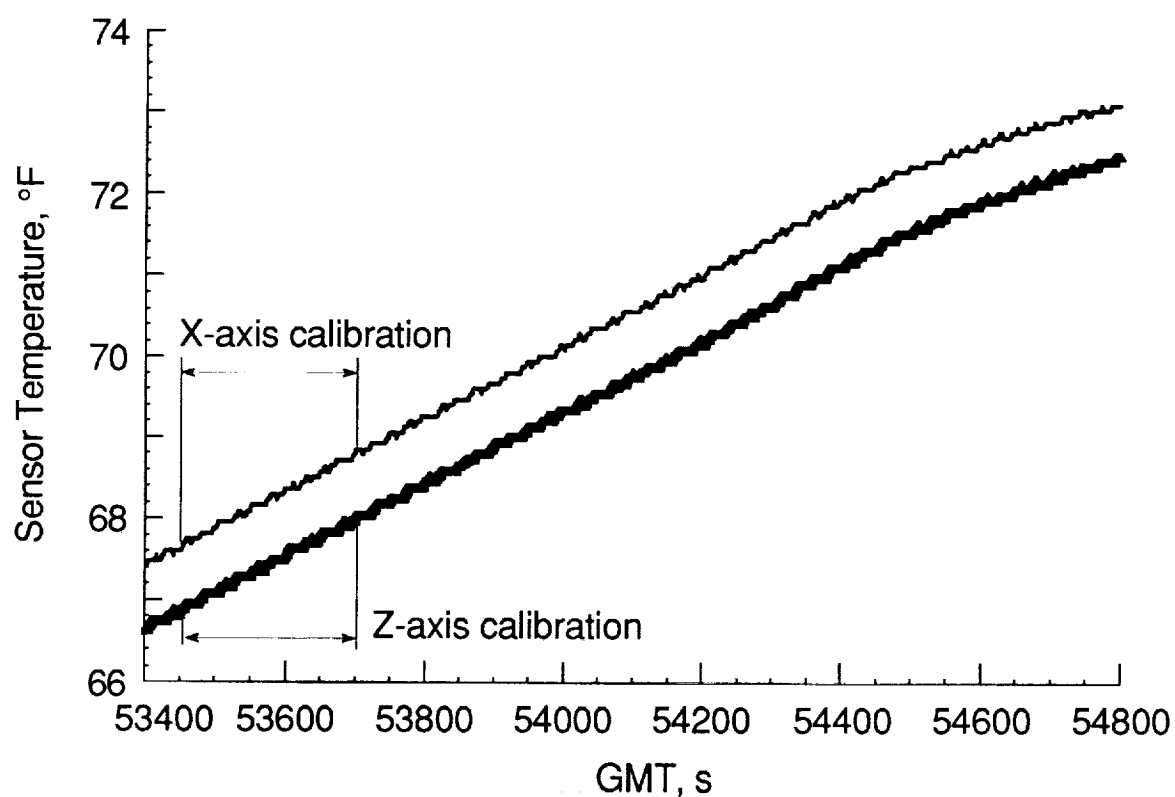


Figure 10. HiRAP STS-40 Acceleration Model Results.

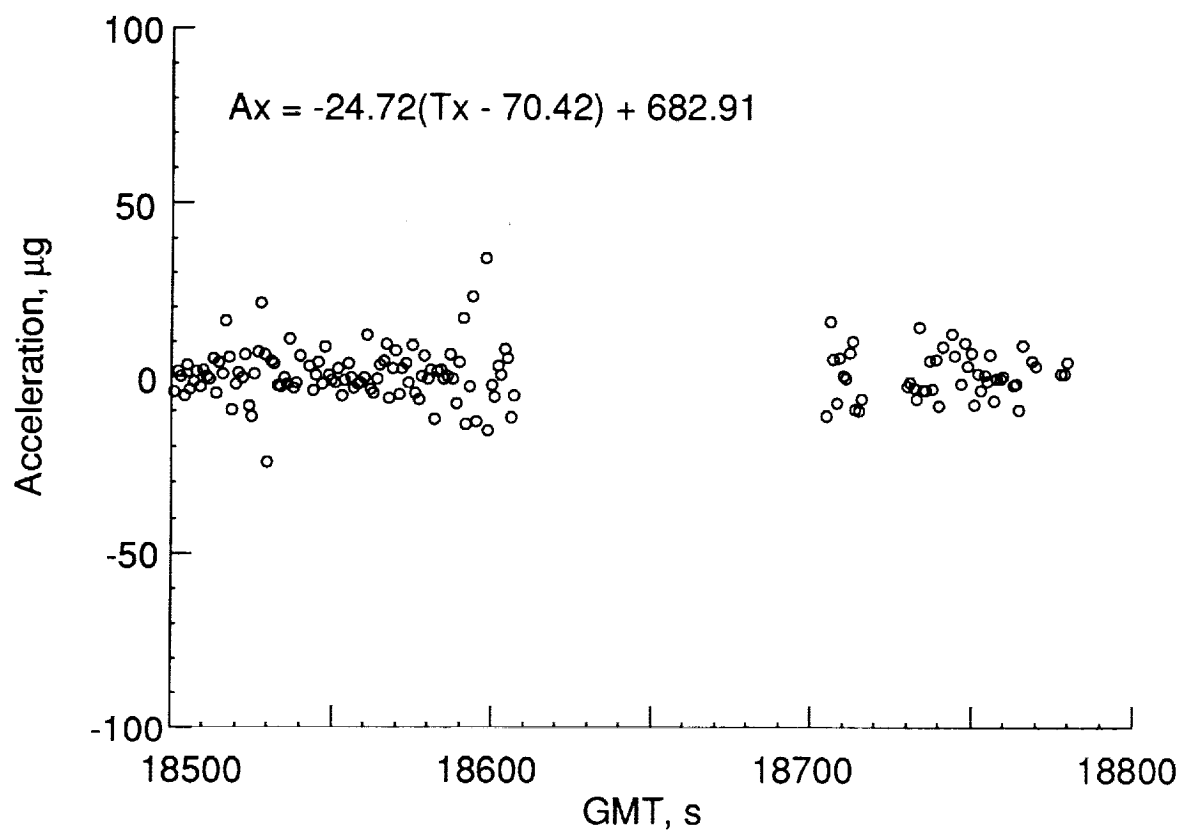


(a) HiRAP STS-35

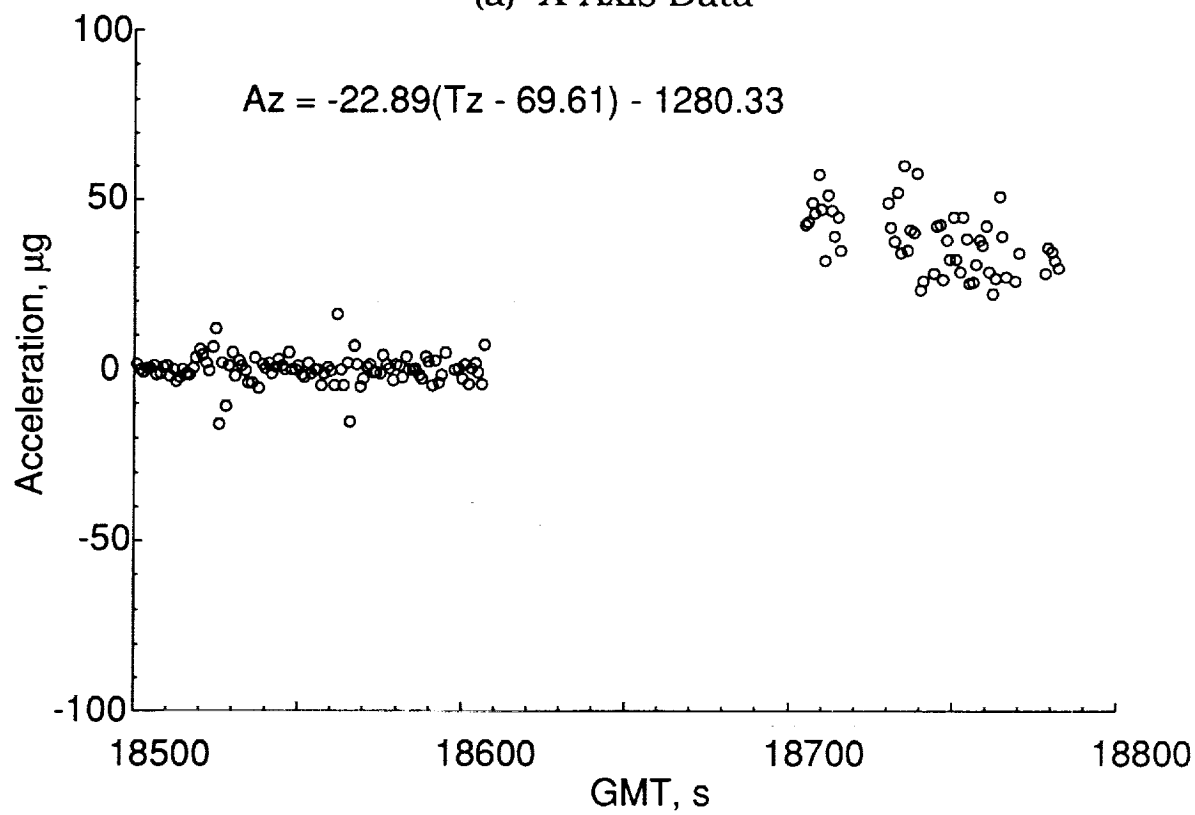


(b) HiRAP STS-40

Figure 11. HiRAP Flight Sensor Temperature Profiles

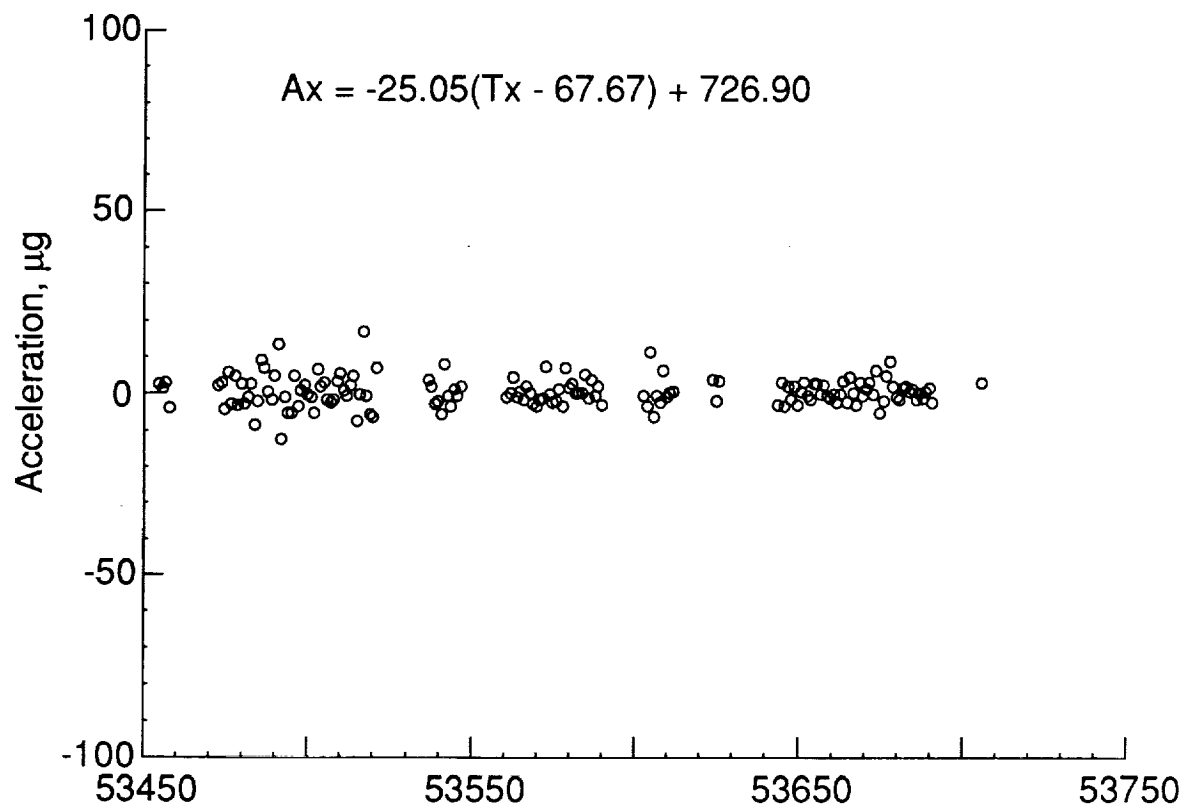


(a) X-Axis Data

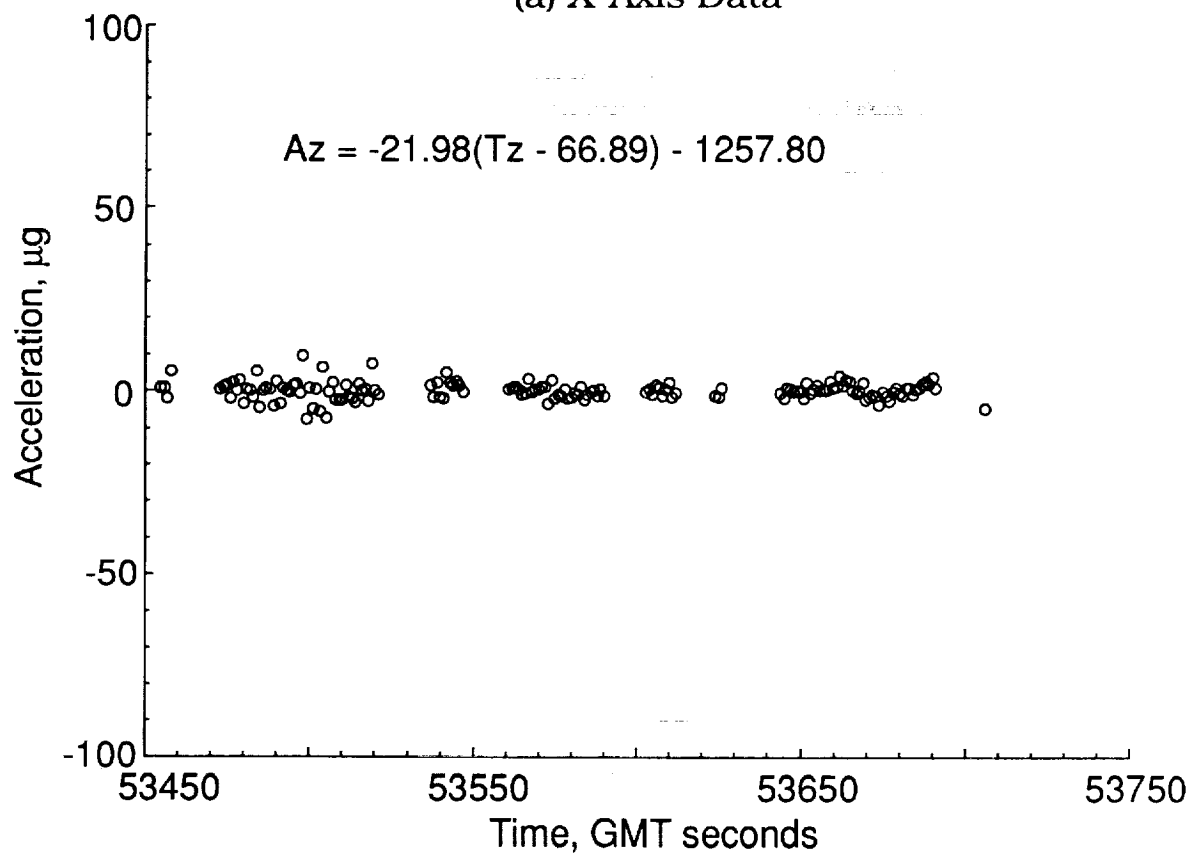


(b) Z-Axis Data

Figure 12. HiRAP STS-35 Flight Calibration Data



(a) X-Axis Data



(b) Z-Axis Data

Figure 13. HiRAP STS-40 Flight Calibration

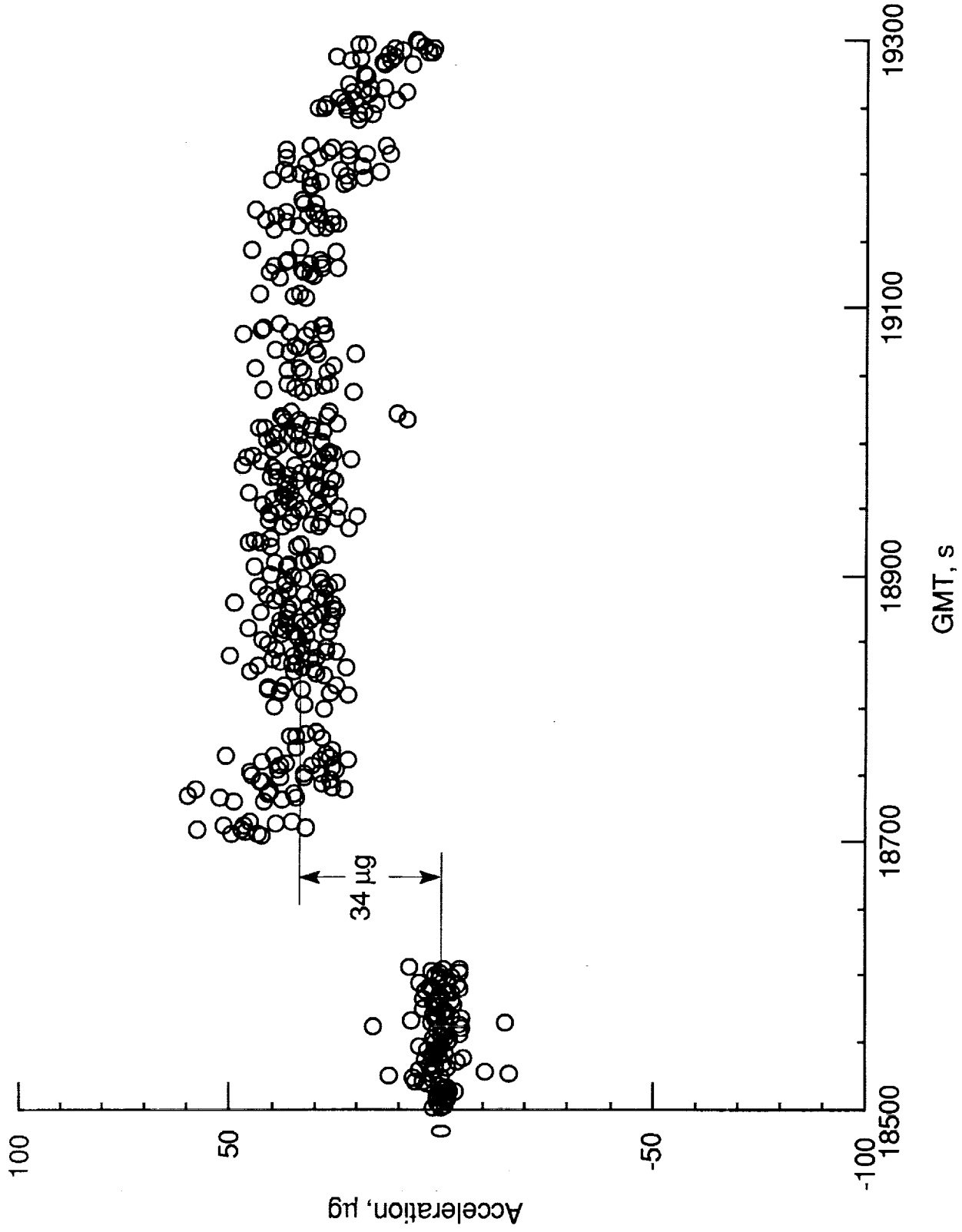


Figure 14. HiRAP STS-35 Z-axis APU Acceleration Correction

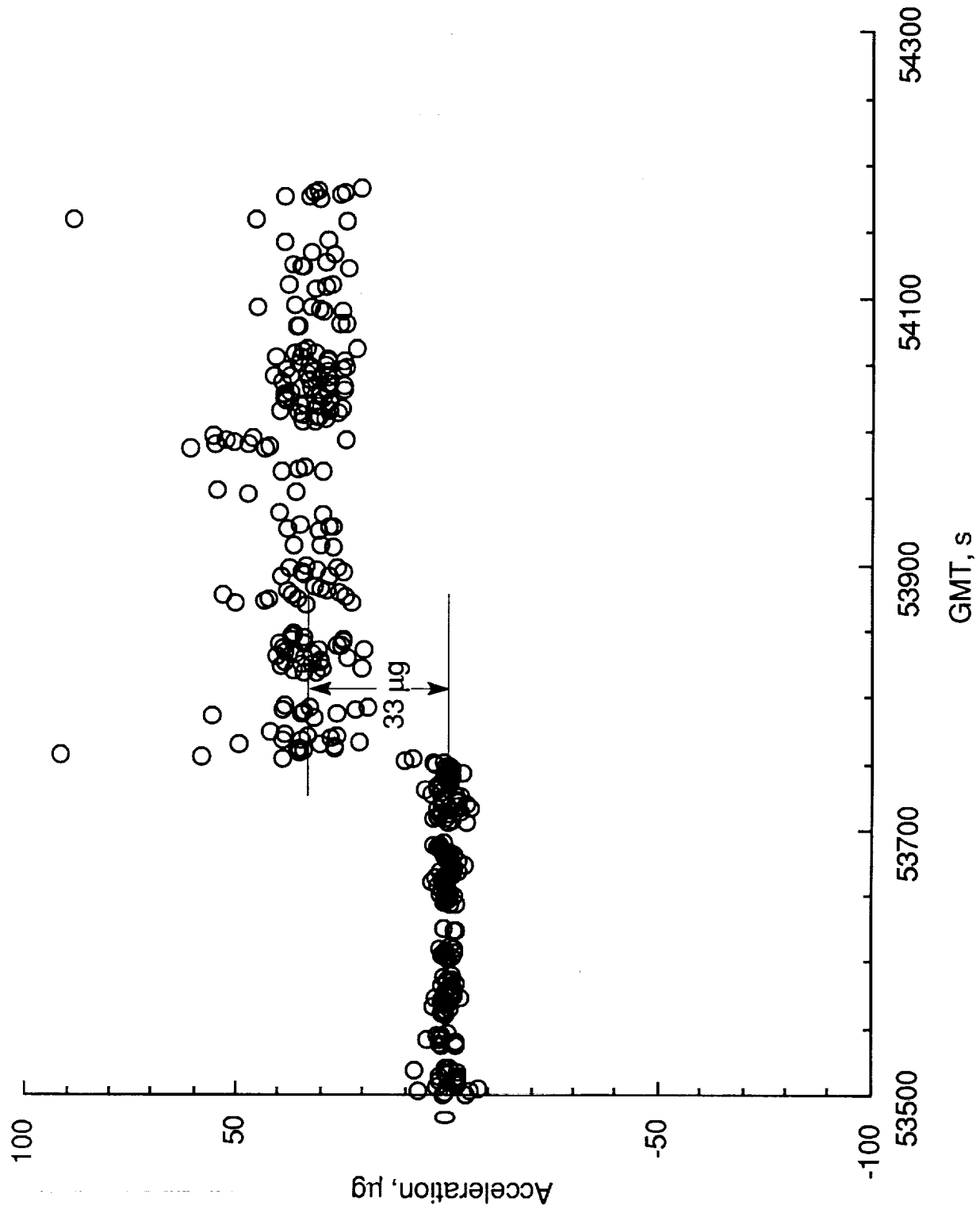


Figure 15. HiRAP STS-40 Z-axis APU Acceleration Correction

REPORT DOCUMENTATION PAGE

Form Approved
OMB No. 0704-0188

Public reporting burden for this collection of information is estimated to average 1 hour per response, including the time for reviewing instructions, searching existing data sources, gathering and maintaining the data needed, and completing and reviewing the collection of information. Send comments regarding this burden estimate or any other aspect of this collection of information, including suggestions for reducing this burden, to Washington Headquarters Services, Directorate for Information Operations and Reports, 1215 Jefferson Davis Highway, Suite 1204, Arlington, VA 22202-4302, and to the Office of Management and Budget, Paperwork Reduction Project (0704-0188), Washington, DC 20503.

1. AGENCY USE ONLY (Leave blank)		2. REPORT DATE April 1992	3. REPORT TYPE AND DATES COVERED Technical Memorandum	
4. TITLE AND SUBTITLE Ground and Flight Calibration Assessment of HiRAP Accelerometer Data From Missions STS-35 and STS-40			5. FUNDING NUMBERS 506-48-11-05	
6. AUTHOR(S) Robert C. Blanchard, Kevin T. Larman, and Christina D. Moats				
7. PERFORMING ORGANIZATION NAME(S) AND ADDRESS(ES) NASA Langley Research Center Hampton, VA 23665-5225			8. PERFORMING ORGANIZATION REPORT NUMBER	
9. SPONSORING/MONITORING AGENCY NAME(S) AND ADDRESS(ES) National Aeronautics and Space Administration Washington, DC 20546-0001			10. SPONSORING/MONITORING AGENCY REPORT NUMBER NASA TM-107602	
11. SUPPLEMENTARY NOTES Blanchard: Langley Research Center, Hampton, VA; Larman: Lockheed Engineering & Sciences Co., Hampton, VA; and Moats: Lockheed Engineering & Sciences Co., Hampton, VA.				
12a. DISTRIBUTION/AVAILABILITY STATEMENT Unclassified-Unlimited Subject Category 19			12b. DISTRIBUTION CODE	
13. ABSTRACT (Maximum 200 words) A method of removing non-aerodynamic signals and calibrating the High Resolution Accelerometer Package (HiRAP) flight data has been developed and is discussed for Shuttle Orbiter missions STS-35 and STS-40. These two mission data sets have been analyzed using ground (dynamic) calibration data and flight calibrations using a flight calibration technique which has been developed and refined over the HiRAP operational lifetime. This technique has evolved early in the flight program since it was recognized that ground calibration factors are insufficient to determine absolute low-acceleration levels. The application of flight calibration factors to the data sets from these missions produced calibrated acceleration levels within an accuracy of less than $\pm 1.5 \mu g$ of zero during a time in the flight when the acceleration level was known to be less than $1 \mu g$. This analysis further confirms the theory that flight calibrations are required in order to obtain the absolute measurement of low-frequency, low-acceleration flight signals.				
14. SUBJECT TERMS Flight accelerometers, calibration techniques, micro-gravity accelerations, and accelerometer measurements			15. NUMBER OF PAGES 30	
			16. PRICE CODE A03	
17. SECURITY CLASSIFICATION OF REPORT Unclassified	18. SECURITY CLASSIFICATION OF THIS PAGE Unclassified	19. SECURITY CLASSIFICATION OF ABSTRACT	20. LIMITATION OF ABSTRACT	